Recruitment dynamics of GAK and auxilin to clathrin-coated pits during endocytosis

Dong-won Lee, Xufeng Wu, Evan Eisenberg and Lois E. Greene*

Laboratory of Cell Biology, NHLBI, NIH, Bethesda, MD 20892-0301, USA

*Author for correspondence (e-mail: greenel@helix.nih.gov)

Accepted 9 June 2006
Journal of Cell Science 119, 3502-3512 Published by The Company of Biologists 2006
doi:10.1242/jcs.03092

Summary

Cyclin G-associated kinase (GAK), the ubiquitous form of the neuronal-specific protein auxilin 1, is an essential cofactor for Hsc70-dependent uncoating of clathrin-coated vesicles. Total internal reflectance microscopy was used to determine the timing of GAK binding relative to dynamin and clathrin binding during invagination of clathrin-coated pits. Following transient recruitment of dynamin to the clathrin puncta, large amounts of GAK are transiently recruited. GAK and clathrin then disappear from the evanescent field as the pit invaginates from the plasma membrane and finally these proteins disappear from the epifluorescence field, probably as the clathrin is uncoated from the budded vesicles by Hsc70. The recruitment of GAK is dependent on its PTEN-like domain, which we found binds to phospholipids. This suggests that interaction with phospholipids is essential for recruitment of GAK and, in turn, Hsc70, but Hsc70 recruitment alone might not be sufficient to induce irreversible clathrin uncoating. When budding of clathrin-coated pits is inhibited by actin depolymerization, there is repeated flashing of GAK on the clathrin-coated pit but neither scission nor irreversible uncoating occur. Therefore, budding as well as synchronous recruitment of GAK might be required for irreversible clathrin uncoating.

Supplementary material available online at
http://jcs.biologists.org/cgi/content/full/119/17/3502/DC1

Key words: GAK, Auxilin, Clathrin, Dynamin, TIRF

Introduction

Clathrin-mediated endocytosis is one of the major mechanisms employed by cells for receptor internalization. Cargo-specific adaptors function to concentrate receptors in the clathrin-coated pits (CCPs). The CCPs then progressively invaginate, their necks contract, and they undergo scission from the plasma membrane to form clathrin-coated vesicles (CCVs). Finally, the CCVs are uncoated and transported into the cell where they fuse with early endosomes. Our laboratory has studied in detail the function of the molecular chaperone Hsc70 and its co-chaperones, either neuronally expressed auxilin or ubiquitously expressed GAK, in endocytosis (Ungewickell et al., 1995; Greener et al., 2000; Umeda et al., 2000). These co-chaperones are members of the J-domain class of proteins, which function to present substrate to Hsc70 (Schlossman et al., 1984; Greene and Eisenberg, 1990). Although Hsc70 was initially thought to be only involved in clathrin uncoating, recent studies have suggested that it also is involved in earlier steps in the endocytic cycle (Newmyer et al., 2003; Lee et al., 2005).

The timing of the events that occur during endocytosis has been elucidated using live cell imaging. This work was pioneered by the initial finding that clathrin light chain labeled with GFP can be used to follow the dynamics of clathrin-mediated endocytosis in living cells (Gaidarov et al., 1999). Since this study, many proteins involved in clathrin-mediated endocytosis have been expressed with fluorophores to obtain the relative timing of their interaction with the budding CCPs. The first step in endocytosis is recruitment of proteins to the plasma membrane to form CCPs. The phosphatidylinositol (4,5)-bisphosphate [PtdIns(4,5)P_2] level on the plasma membrane plays a key role in this recruitment (Wenk and De Camilli, 2004) but it is still unclear what causes the PtdIns(4,5)P_2 level to locally increase when a CCP begins to form. In a recent study, Ehrlich et al. used a spinning-disc confocal microscope to show that clathrin, AP2 and dynamin were all recruited with the same time course to newly forming pits (Ehrlich et al., 2004). The pits appeared to initiate randomly on the plasma membrane but about one-fourth of the nascent pits aborted before invagination. Interestingly, in a recent study where GAK was depleted from the cell by RNA interference (RNAi), we found that Hsc70 is also required for the formation of nascent pits; Hsc70 not only chaperoned clathrin, but also the adaptors AP2 and epsin so that they could bind to nascent pits (Lee at al., 2005).

Once CCPs form on the plasma membrane, membrane curvature must occur as the pits invaginate. Although in vitro studies have suggested that both epsin and AP2 alter the curvature of the membrane it is still unclear exactly what role is played by these membrane-binding proteins as opposed to the clathrin coat itself, which may also actively induce membrane curvature (Ford et al., 2001; Ford et al., 2002). In this regard, in vivo studies have shown that clathrin exchange occurs on the CCPs during endocytosis and this exchange may play a role in changing the curvature of the clathrin coat as CCPs invaginate (Wu et al., 2001). Since both in vivo and in vitro studies have shown that Hsc70 and GAK are required for clathrin exchange (Yim et al., 2005; Lee et al., 2005), Hsc70

might be involved in the ATP-dependent changes in clathrin-coat curvature that occur as CCPs invaginate.

Following invagination, the next steps in formation of CCVs is constriction of the CCP necks followed by scission of the newly formed CCVs from the plasma membrane. It is generally agreed that a key protein involved in both constriction and scission is the large GTPase dynamin, which polymerizes into rings that constrict as dynamin hydrolyzes GTP (Hinshaw, 2000). It has also been suggested that auxilin and Hsc70 play a role in the constriction and scission steps. This is based on the studies of Newmyer et al., in which they found that auxilin bound to dynamin (Newmyer et al., 2003). Moreover, fragments of auxilin inhibited endocytosis and this inhibition can be overcome by excess dynamin.

In addition to dynamin, actin has also been suggested to have a role in scission. The roles of dynamin and actin have been studied in detail using total internal reflectance fluorescence (TIRF) microscopy in which the evanescent field illuminates the basolateral surface of the cell. Using this technique, dynamin fluorescence was shown to reach a peak and then sharply decrease either just prior to (Merrifield et al., 2002) or at the same time as clathrin-fluorescence intensity declines (Rappoport and Simon, 2003). When CCP dynamics were followed simultaneously in the evanescent and epifluorescence fields, Merrifield et al. observed that clathrin disappeared from the epifluorescence field about 30 seconds after it disappeared from the evanescent field (Merrifield et al., 2002); also during the period of decreasing dynamin and clathrin intensity, actin, Arp2/3 and cortactin were recruited to the CCPs (Merrifield et al., 2002; Merrifield et al., 2004; Merrifield et al., 2005). Depolymerization of actin has been shown to inhibit clathrin budding (Moskowitz et al., 2003; Yarar et al., 2005; Merrifield et al., 2005). However, these studies do not show whether actin by itself causes scission or, whether scission is mainly driven by dynamin when actin or other motility proteins exert tension on the constricted neck of the budding vesicle (Roux, 2006).

Following scission, the CCVs they must be uncoated before they can fuse with early endosomes. In addition to the strong evidence that GAK and Hsc70 are involved in clathrin uncoating, there is evidence that the PtdIns(4,5)P_2 phosphatase synaptojanin also plays a role in clathrin uncoating (Cremona et al., 1999). Although clathrin does not bind directly to PtdIns(4,5)P_2, synaptojanin might affect clathrin binding by controlling the binding of adaptors, such as AP2, that do bind to PtdIns(4,5)P_2. However, there is still controversy on whether AP2 is even present on the budded CCV or whether it remains behind on the plasma membrane after budding (Rappoport et al., 2003; Keyel et al., 2004, Rappoport et al., 2005). Therefore, the relative roles of synaptojanin and Hsc70 in the uncoating of CCV remain to be determined.

Since GAK and Hsc70 are involved in reversible clathrin exchange during invagination, an interaction with dynamin during constriction and irreversible clathrin uncoating after scission, the timing of GAK recruitment to CCPs is likely to be highly regulated. We therefore used TIRF microscopy to determine the timing of GFP-GAK recruitment relative to that of dynamin and clathrin in living cells. Although we could not detect GAK on the CCPs prior to dynamin recruitment, we found that, following dynamin recruitment, there is a wave of GAK recruitment, and shortly thereafter both clathrin and GAK disappear from the evanescent field. This is followed by the simultaneous disappearance of clathrin and GAK from the epifluorescence field, presumably when clathrin uncoating occurs. We conclude that a low level of GAK on the CCPs is sufficient to catalytically support the reversible clathrin exchange that occurs before vesicle budding, whereas recruitment of large amounts of GAK are necessary for the irreversible clathrin uncoating that occurs after CCV scission.

Results

Recruitment of GAK and auxilin to CCPs

To examine GAK localization in living cells, CV1 and HeLa cells were transfected with GFP-GAK. The transfected cells showed pronounced perinuclear localization of GAK and a cytosolic pool of GAK. To reduce background fluorescence, we only imaged cells whose GFP intensity was barely visible by eye when viewed in the epifluorescent field. This population of cells showed no difference from control cells in uptake of Alexa-Fluor-546-transferrin (data not shown). By contrast, cells that had relatively high GFP intensity in the epifluorecent field showed a reduction of transferrin uptake, consistent with our previous finding that inhibition of clathrin-mediated endocytosis only occurs when GAK is highly overexpressed (Zhao et al., 2001). When viewing the dim cells in the evanenscent field, green flashes of GAK were visible all over the plasma membrane (see supplementary material, Movie 1).

Although the flashing of GAK was clearly visible by TIRF microscopy, it was difficult to detect flashing of GFP-GAK on the plasma membrane when cells were imaged using confocal microscopy. The TIRF microscope uses a CCD camera to acquire images, whereas the confocal microscope acquires images by line scanning so that acquisition time is much slower with the confocal microscope. In addition to the longer imaging times, the transient nature of the GAK flashes, the wider depth of field and the presence of diffuse cytosolic GAK, all contributed to the poor resolution of GFP-GAK when imaged by confocal microscopy. We also tried to detect GAK on the plasma membrane by immunostaining. Imaging of HeLa or CV1 cells immunostained for GAK showed no detectable GAK on the plasma membrane by either TIRF or confocal microscopy, presumably because the binding of high levels of GAK to CCPs on the cell surface is transient. GAK did show pronounced perinuclear staining, presumably associated with the Golgi because it colocalized with Golgi markers such as GGA3, AP1, TGN38 and GM130 (data not shown).

To determine the relationship between the GAK flashes and clathrin-mediated endocytosis, CV1 cells were co-transfected with the constructs monomeric red fluorescent protein (mRFP) fused to clathrin light chain A (LCa) (mRFP-clathrin LCa) and green fluorescent protein (GFP) fused to GAK (GFP-GAK), and imaged simultaneously using the TIRF microscope equipped with an optical beam splitter (Fig. 1A). Movie 2 shows that GAK was occurring on clathrin puncta but, at any given time, less than 5% of the puncta showed GAK flashes (see supplementary material, Movie 2). Both CV1 and HeLa cells showed a similar relationship of GAK occurrences and RFP-clathrin puncta. Moreover, we obtained similar results with DsRed-clathrin LCa but we generally used the monomeric RFP construct rather than the tetrameric DsRed-construct in our studies.

Analysis of 100 GAK flashes from five CV1 cells using Metamorph software showed that >95% of the flashes occurred

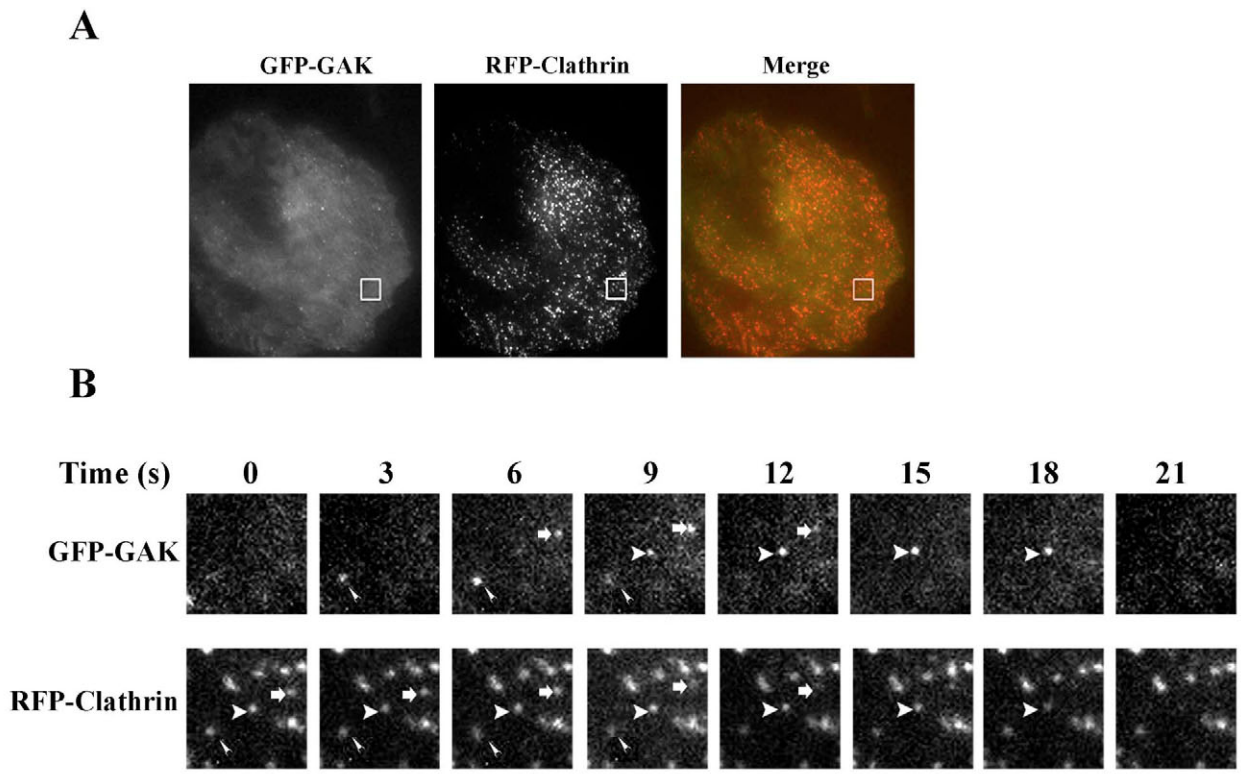

Fig. 1. TIRF microscopy images of a CV1 cell co-transfected with GFP-GAK and mRFP-clathrin. (A) A CV1 cell was simultaneously imaged for GFP-GAK (left) and mRFP-clathrin (middle) and images were merged (right). (B) Magnified time-lapse sequence of boxed areas from GFP-GAK and mRFP-clathrin images of A showing the behavior of GAK and clathrin. GAK and its corresponding clathrin puncta are indicated by the arrow, arrowhead and pointer.

on clathrin puncta. In 77% of the flashing events, the clathrin puncta disappeared within 10 seconds after the flash of GFP-GAK fluorescence. An expanded region of the cell in Fig. 1B illustrates that the flash of GAK fluorescence precedes the disappearance of clathrin. Clathrin did not show any change in intensity in 13% of the flashing events, whereas in 10% of the flashing events, clathrin showed a 25-50% decrease in fluorescence intensity following the flash. This partial drop in fluorescence intensity might have occurred because of the loss of a single CCP from a cluster of pits.

We next identified disappearing clathrin puncta to determine whether in all cases, a GAK flash preceded the disappearance of clathrin puncta. Analysis of 50 disappearing clathrin puncta showed that only half were preceded by a GAK flash, suggesting that there are at least two classes of disappearing clathrin puncta. This effect might be related to the recent observation that, in addition to the mature pits that undergo endocytosis, there is a population of nascent puncta that disintegrate prior to reaching maturity (Ehrlich et al., 2004). To select for a population enriched in mature pits undergoing clathrin-mediated endocytosis, we selected puncta that showed at least a twofold increase in clathrin fluorescence intensity prior to their disappearance. By examining 18 such puncta, we found that all of them showed a GAK flash. Therefore, these results suggest that the GAK flash occurs on mature CCPs before they disappear from the evanescent field.

Time series of TIRF images were analyzed to determine the duration of the flash of GAK fluorescence and its relationship to clathrin fluorescence. Plotting the fluorescence intensity of GAK as a function of time, we found that GAK is associated with the clathrin puncta on the plasma membrane for 11.6±3 seconds (Fig. 2A, ●). Auxilin, the neuronal-specific homolog of GAK, showed a similar time course of recruitment to the plasma membrane, remaining associated with the plasma membrane for 10.7±3 seconds (Fig, 2A, ○). Fig. 2B,C shows the relative timing of the fluorescence change of clathrin with respect to GAK and auxilin, respectively. Following the flash of either GAK or auxilin, both proteins disappear from the evanescent field with the same time course as clathrin.

As CCPs invaginate, the clathrin fluorescence shows a steep drop in intensity. By taking the time point at the start of this decline, we can calculate the time interval between the onset of the clathrin fluorescence decline and the time the GAK and auxilin fluorescences reach maximum intensity. To determine this time interval, individual events were analyzed and the resulting data plotted on histograms (Fig. 3A,B). These plots show that the peaks of GAK and auxilin fluorescence occurred after the onset of the decline in clathrin fluorescence intensity. For both GAK and auxilin, the median of the flash peaks occurred 7 seconds after clathrin fluorescence started to decline, showing that the peaks of GAK and auxilin fluorescence intensity occur well into the invagination process.

After measuring the timing of GAK fluorescence relative to clathrin fluorescence during the invagination process, we next measured the timing of dynamin fluorescence relative to clathrin fluorescence. TIRF microscopy was used to examine

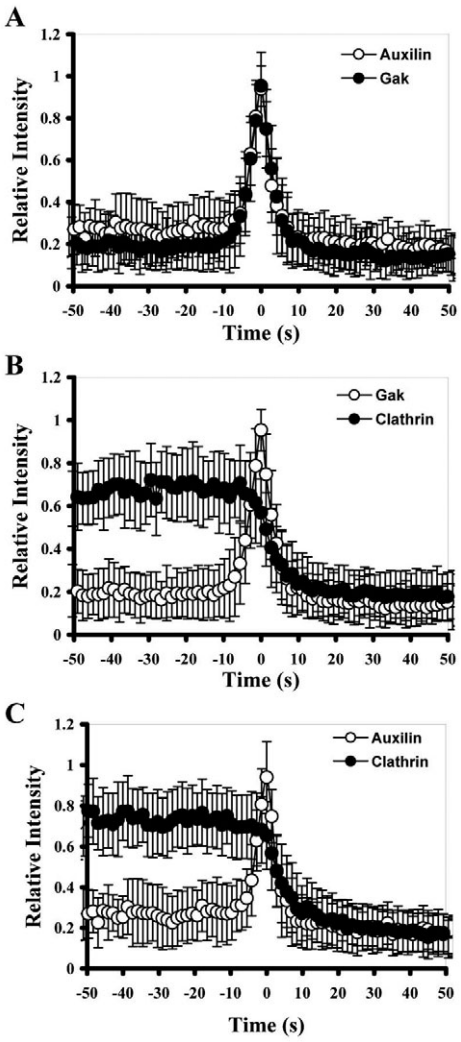

Fig. 2. Recruitment of GAK or auxilin to CCPs. Fluorescence intensity of GFP-GAK and mRFP-clathrin observed under a TIRF microscope was analyzed by Metamorph as described in the Materials and Methods. (A) Time course of the change in fluorescence intensities of GFP-GAK (●) and GFP-auxilin (○). (B) Change in fluorescence intensities of GFP-GAK (○) and mRFP-clathrin (●) as a function of time; measured from 56 puncta in 9 cells. (C) Change in fluorescence intensities of GFP-auxilin (○) relative to mRFP-clathrin (●) as a function of time; measured from 41 puncta in 7 cells. Sequential images were taken one frame per second for 2 minutes. The zero time point was set to the time at which the GAK or auxilin reached its maximum.

cells co-transfected with the GFP-fusion construct, GFP-dynamin1 or GFP-dynamin2, and mRFP-clathrin LCa. The plots of clathrin and dynamin fluorescence showed that we obtained similar time courses for both dynamin1 and dynamin2 (Fig. 4). In both cases, dynamin bound to the pit just prior to invagination. By contrast, Rappoport and Simon found, using MDCK cells, that dynamin2 but not dynamin 1 associated with the pit prior to invagination (Rappoport and Simon, 2003). The difference in our results and those of Rapapport and Simon for dynamin2 may be because of our use of CV1 cells as opposed to MDCK cells.

Following the recruitment of dynamin to the CCP, the clathrin and the dynamin fluorescence intensities decreased. The timing interval was measured between the onset of the clathrin fluorescence decline and the dynamin fluorescence peaks. As shown in Fig. 3, the median value between the onset of the clathrin decline and the dynamin1 peak was 0 seconds, whereas this value was 1 second for dynamin2. These results are similar to the TIRF studies in which the peaks of clathrin and dynamin1 (or dynamin2) fluorescence occurred simultaneously in MDCK cells (Rapport and Simon, 2003). A slightly different time course was observed in Swiss 3T3 cells in which the peak of the GFP-dynamin1 fluorescence was found to slightly precede the decline in clathrin fluorescence (Merrifield et al., 2002).

Since our results showed that the onset of the clathrin fluorescence decline coincided with the fluorescence peaks of dynamin1 and dynamin2 but preceded the GAK and auxilin peaks (Fig. 3A,B), if dynamin and GAK fluorescence were measured simultaneously, the peak of the dynamin fluorescence should precede the peak of the GAK fluorescence. This was tested by directly measuring the time interval between the dynamin1 and GAK peaks in CV1 cells co-transfected with GFP-GAK and mRFP-dynamin1. Fig. 5A, a typical plot of the fluorescence intensities of these proteins as a function of time, shows that the dynamin fluorescence peak indeed precedes the GAK fluorescence peak by 11 seconds. The histogram in Fig. 5B from 32 events shows that the dynamin1 fluorescence peak preceded the GAK fluorescence peak in more than 90% of the events, although there was a wide distribution in the time interval. The median time interval between the dynamin1 peak and the GAK peak was 16 seconds. These results are consistent with the histogram data in Fig. 4 showing that dynamin is recruited to the CCP prior to GAK.

The decrease in clathrin fluorescence in the evanescent field has been attributed to invagination of the CCP. Epifluorescence microscopy has a much greater depth of field than TIRF microscopy. We therefore used epifluorescence microscopy to determine whether the flash of GAK is associated with clathrin uncoating. CV1 cells, co-transfected with GFP-GAK and mRFP-clathrin LCa, were imaged over time using epifluorescence microscopy (supplementary material, Movie 3). As expected, there is much greater background noise in these epifluorescence experiments but, nevertheless, we could detect that the GAK and clathrin fluorescence signals disappeared simultaneously from the epifluorescence field (Fig. 6A). To relate the events occurring in the cytosol to those that occur on the plasma membrane, CV1 cells were imaged alternating between the epifluorescence and evanescent fields of illumination. The change in fluorescence of GAK and clathrin were plotted using images obtained for the same set of events in the evanescent field (Fig. 6B) and the epifluorescent field (Fig. 6C). Overall, the plots look quite similar but, as expected, it takes longer for the clathrin and GAK to disappear from the epifluorescent field than the evanescent field. Since CV1 cells are rather flat, especially at the cell periphery, the loss of fluorescence from the epifluorescence field most probably corresponds to CCV uncoating rather than the CCVs disappearing into the interior of the cell. Preliminary results using very fast 3D-imaging (four frames per second) also showed that the clathrin and GAK fluorescence signals both disappeared within 1 second of one another. Taken together,

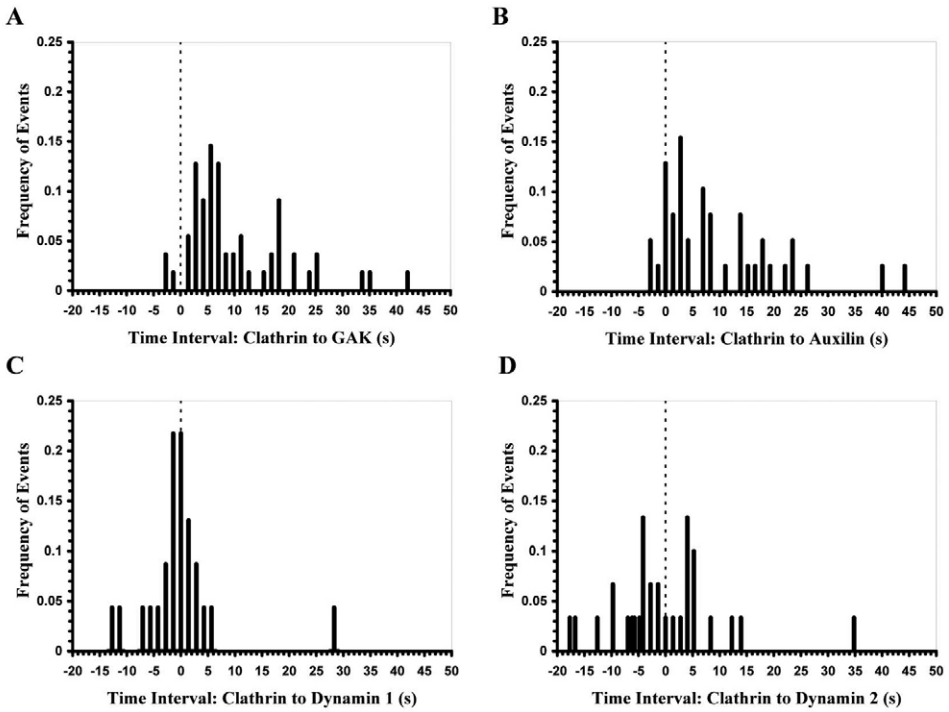

Fig. 3. Histograms showing the time interval between the clathrin and the peaks of GAK and auxilin. (A) Time interval between clathrin and GAK peaks, calculated from the events used in Fig. 2B. (B) Time interval between clathrin and auxilin peaks, calculated from the events used in Fig. 2C. (C) Time interval between clathrin and dynamin1 peaks, calculated from the events used in Fig. 4A. (D) The time interval between clathrin and dynamin2 peaks, calculated from the events in Fig. 4B. In calculating the peak of maximum clathrin fluorescence in the histograms, the fluorescence data were fitted using Microsoft Excel and a moving average of four to reduce noise in the clathrin data.

our results suggest that GAK is recruited after CCP invagination begins, and then is involved in clathrin uncoating as well as perhaps vesicle scission after the CCVs have invaginated from the plasma membrane.

GAK- and auxilin-domains, and lipid binding

Since GAK and auxilin are both multi-domain proteins that interact with several components of the CCP, truncations of these proteins were made to determine which domains are required for the GAK and auxilin flashes. When imaged by confocal microscopy all of the different constructs had comparable levels of fluorescence, showing they were expressed at approximately the same level. As discussed previously, we selected dim green cells to image in our TIRF microscopy studies to avoid problems due to background fluorescence and clathrin sequestration (Zhao et al., 2001). Fig. 7 summarizes the behavior of the constructs that we tested. Quantification was done by counting the number of flashes that occur in a fixed area over a 10-second period. As expected, because both auxilin and GAK flash, deleting the kinase domain of GAK had no effect on the flashing. The C-terminal J-domain of GAK was also not essential for flashing. Our data show that the extent of flashing of the J-domain deletion mutant was the same as for full-length GAK. Since this J-domain-deletion mutant was expressed at low levels in cells that also contain endogenous GAK, it would not be expected to act as a dominant-negative inhibitor. We also deleted residues 752-979 of GAK, a region that is homologous to the region of auxilin, which was identified as the major dynamin binding site (Newmyer et al., 2003). Whereas this large deletion did abolish GAK flashing, it should be noticed that this region also contains clathrin and AP2-binding sites (Scheele et al., 2001).

Truncation of GAK to delete the PTEN-like domain and the adjacent N-terminal kinase domain also resulted in loss of flashing. Extensive mapping of the PTEN-like domain was done and the region crucial to flashing was narrowed to amino acid residues 384-405, a very hydrophilic region (Fig. 7). We mutated the residues in this region that are common to both GAK and auxilin. Mutation of the conserved leucine residue L389 to aspartic acid was found to completely eliminate flashing (Fig. 7). This does not appear to be just an effect of charge because the mutation of the conserved lysine K390 to glutamic acid did not eliminate flashing. We also found that the secondary structure of the PTEN-like domain has a role in flashing. Deletion of residues 310-384, the N-domain (N-terminal auxilin-homology region) between the kinase domain and the PTEN-like domain, prevented flashing but a complete truncation of residues 1 to 384 did not, presumably because the kinase domain no longer interfered with the PTEN-like domain. Of course, the larger truncation of residues 1-405 prevented flashing because, in this case, the crucial hydrophilic PTEN-like domain itself was deleted. Finally, a construct of GAK consisting of just the kinase and PTEN-like domains did not flash, showing that the C-terminal domain, which contains the clathrin-, AP2- and dynamin-binding sites, is also necessary for the binding of GAK to CCPs.

We also analyzed the domains of auxilin essential for the flashing of auxilin on CCPs. In auxilin, amino acids 38-59 span the hydrophilic region that is homologous to the essential region in GAK that is necessary for flashing. Surprisingly, however, in contrast to GAK, deletion of the entire PTEN-like domain of auxilin (Δ1-218) just reduced the flashing of auxilin but did not eliminate it. However, a smaller truncation of the PTEN-like domain, Δ1-59, did eliminate flashing, and Δ1-196 very markedly reduced it. These results suggest that when fragments of the PTEN-like domain are present they inhibit the binding activity of the adjacent C-terminal domain. Since total

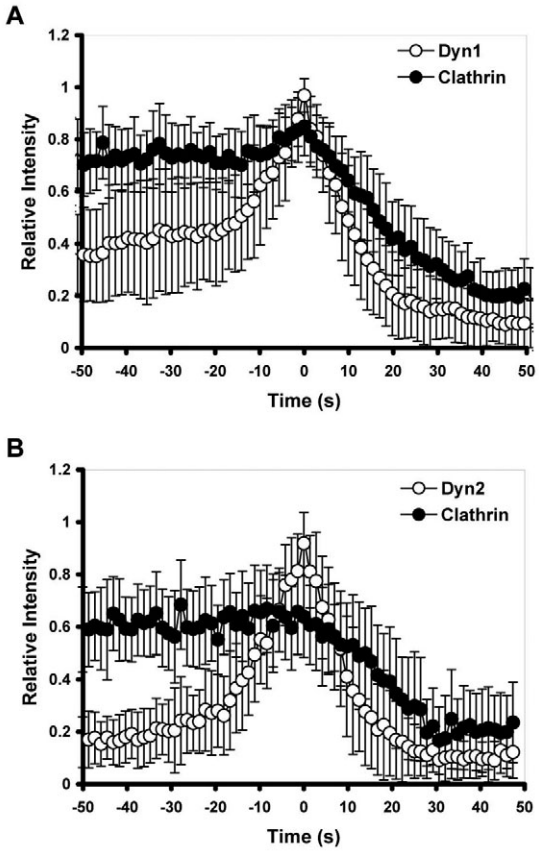

Fig. 4. Recruitment of dynamin1 or dynamin2 to CCPs in CV1 cells. Fluorescence intensity of GFP dynamin and mRFP-clathrin observed under TIRF microscopy was analyzed by Metamorph as described in the Materials and Methods. (A) The change in fluorescence intensities of GFP-dynamin1 and mRFP-clathrin as a function of time measured from 25 puncta in 7 cells. (B) The change in fluorescence intensities of GFP-dynamin2 and mRFP-clathrin as a function of time measured from 32 puncta in 5 cells. The zero time point was set to the time at which dynamin reached its maximum.

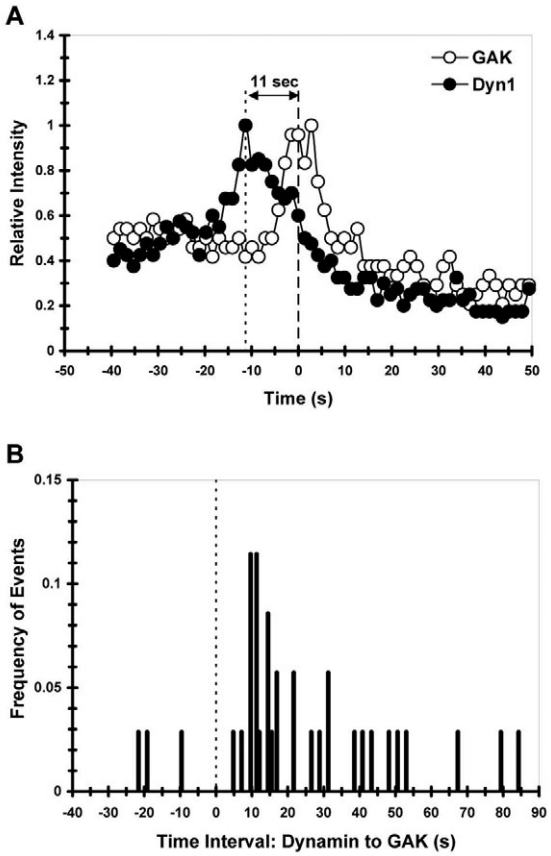

Fig. 5. Recruitment of dynamin 1 and GAK to the plasma membrane. CV1 cells were co-transfected with GFP-GAK and mRFP-dynamin 1. Metamorph analysis was used to identify GAK and dynamin colocalizing at the same localization. (A) The changes in fluorescence intensities of dynamin1 (○) and GAK (●) were plotted as a function of time. The difference in times between the maximum of the dynamin 1 and GAK peaks is the time interval plotted in the histogram. (B) Histogram of the time intervals between the maximum dynamin and GAK fluorescence obtained from 32 events in two cells.

elimination of the PTEN-like domain does not prevent auxilin flashing, another region on auxilin, presumably the C-terminal domain, must transiently recruit auxilin to CCPs.

Although the PTEN-like domain of GAK and auxilin shares homology with the phospholipid phosphatase PTEN, some crucial residues at the phosphatase site of PTEN are not conserved in GAK and auxilin. Based on the amino acid homology between the PTEN-like domain and PTEN, it was proposed that, in auxilin, this domain would bind to but not hydrolyze phospholipids (Haynie and Ponting, 1996). Given the importance of the PTEN-like domain in the transient recruitment of GAK to the CCPs, its ability to bind phospholipids was examined using a lipid overlay assay. The PTEN-like domain of GAK was expressed and purified as a GST-fusion protein and purified. The lipid-overlay assay shows that the PTEN-like domain binds phospholipids (Fig. 8A) and quantification of the overlay shows that this domain preferentially binds to the phosphatidylinositol monophosphates, PtdIns(3)*P*, PtdIns(4)*P* and PtdIns(5)*P*, and to a lesser extent to PtdIns(4,5)P_2 (Fig. 8B).

GAK recruitment under different conditions

We next examined the recruitment of GFP-GAK to the plasma membrane under conditions in which clathrin-mediated endocytosis was blocked by either expressing the dominant-negative K44A-dynamin mutant or depleting the cell of cholesterol. The latter treatment blocks invagination of the pit, whereas the former blocks constriction of the neck, but with both treatments clathrin on the pit still exchanges at about the same rate as in control cells (Wu et al., 2001). When CV1 cells were co-transfected with GFP-GAK and the K44A-dynamin mutant, GAK did not flash nor did it flash in HeLa cells stably expressing the K44A-dynamin mutant (Table 1). However, as expected, overexpression of wild-type dynamin had no effect on GAK flashing in either CV1 or HeLa cells (Table 1). Similar to treatment with the K44A dynamin mutant, cholesterol-depletion prevented GFP-GAK flashing in both CV1 and HeLa cells (Table 1). Therefore, blocking endocytosis by preventing invagination or constriction prevents GAK recruitment.

We also examined whether GAK flashed in cells where clathrin-mediated endocytosis was blocked by K^+-depletion or

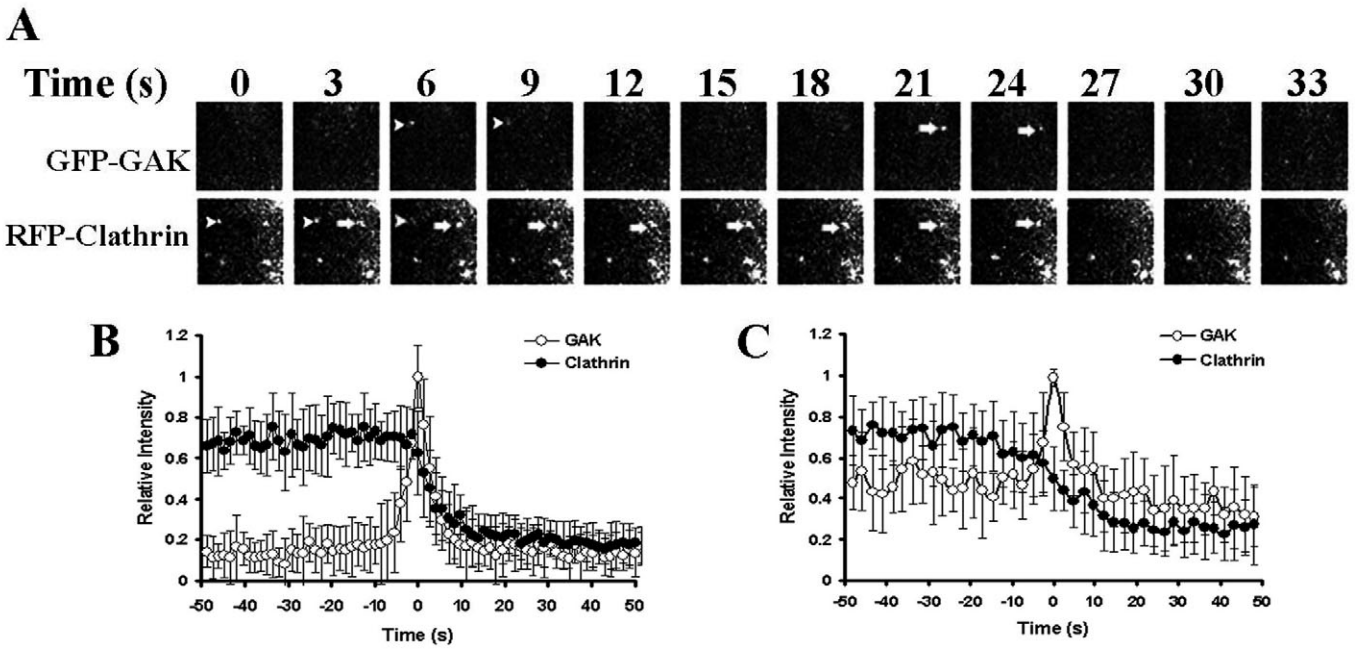

Fig. 6. GFP-GAK and mRFP-clathrin recruitment and disappearance from the plasma membrane imaged using evanescent and epifluorescence microscopy. CV1 cells, co-transfected with GAK and clathrin, were simultaneously imaged at a rate of 1 frame per second for a total of 2 minutes. (A) Epifluorescence images from time-lapse sequence of GFP-GAK and mRFP-clathrin. GAK and its corresponding clathrin puncta are shown by the arrow and arrowhead. (B) Time course of the change in fluorescence intensities of GFP-GAK (○) and mRFP-clathrin (●) imaged in the evanescent field from 11 events in 5 cells. (C) Time course of the change in fluorescence intensities of GFP-GAK (○) and mRFP-clathrin (●) imaged in the epifluorescent field using the same events that were identified in the evanescent field. The data were normalized so that the peak of GAK fluorescence was set to zero.

hypertonic sucrose, conditions which immobilize clathrin on CCPs in addition to blocking endocytosis (Wu et al., 2001). As expected, there was no flashing of GAK under these conditions but, interestingly, GFP-GAK continuously bound to CCPs in many of these cells. This is evident in the kymograph in Fig. 9. For comparison, Fig. 9 also shows a kymograph of GAK flashing in untreated control cells. The continuous binding of GAK to the CCPs in hypertonic-sucrose-treated or K^+-depleted cells was most apparent when the cells were co-transfected with DsRed-clathrin LCa rather than mRFP-clathrin LCa. Interestingly, this continuous binding of GAK occurred even when the GAK construct lacked the PTEN-like domain (data not shown). Although GFP-GAK continuously bound to pits under these conditions, in contrast to clathrin it still exchanged when we measured its fluorescence recovery after photobleaching on the confocal microscope (data not shown), just as we previously observed for other clathrin adaptors in hypertonic-sucrose-treated or K^+-depleted cells (Wu et al., 2003). Therefore, although the PTEN-like domain is required for GAK flashing it is apparently not required to simply recruit GAK to CCPs.

We also examined GAK flashing in HeLa cells in which either clathrin or AP2 was depleted by RNAi and, in both cases, detected no GFP-GAK flashing. It is perhaps not surprising that clathrin-depleted cells showed no GFP-GAK flashing, but we would have expected GAK flashing in AP2-depleted cells because they still have CCPs that take up epidermal growth factor (EGF) and low-density lipoprotein (LDL) (Motley et al., 2003). However, perhaps because these latter cells only have 10% CCPs of control cells and the few remaining puncta are much smaller (Motley et al., 2003), we may have been unable to detect GAK flashing even if it occurred.

Finally, we examined GAK recruitment when cells were treated with latrunculin A (LatA) to depolymerize actin. Actin depolymerization in Swiss 3T3 cells markedly inhibited clathrin budding on the basolateral surface (Yarar et al., 2005; Merrifield et al., 2005), whereas in CHO cells stably expressing human transferrin receptor, LatA treatment caused about a 50% reduction in membrane budding (Moskowitz et al., 2003). We found that, following the flash of GAK, 75% of CCPs did not invaginate from the plasma membrane in LatA-treated CV1 cells. As illustrated in Fig. 9, GFP-GAK showed repeated flashes on the clathrin puncta without loss of clathrin intensity in these treated cells (see arrowheads, Fig. 9). Therefore, although there appeared to be no scission of CCVs in the LatA-treated cells, GAK was recruited to the CCPs. Since GAK flashing occurred in LatA-treated cells, these data show that recruitment of high levels of GAK to CCPs is not by itself sufficient to cause scission or clathrin uncoating.

Discussion

TIRF microscopy has proven to be an excellent technique for studying the timing of endocytic and exocytic events owing to its narrow depth of field at the basolateral surface of the cell. We applied this technique to determine the timing of GAK recruitment to the plasma membrane both under conditions in which active clathrin-mediated endocytosis is occurring and under conditions in which it is blocked. GAK in conjunction with Hsc70 carries out multiple chaperone functions during the endocytic cycle. GAK and Hsc70 are required for clathrin

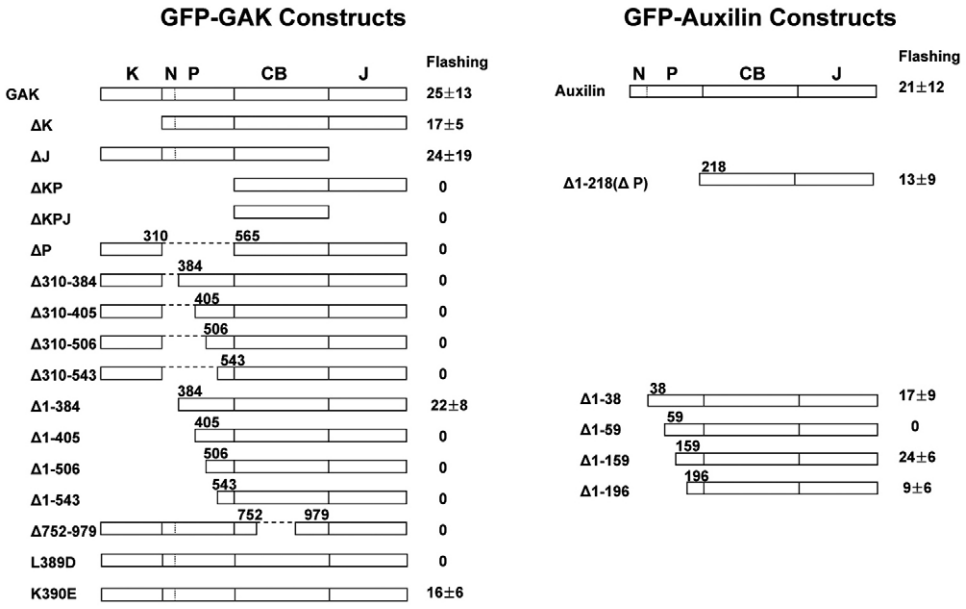

Fig. 7. Mutational analysis of the flashing requirements of GAK and auxilin. Different GFP constructs of GAK and auxilin were transfected into CV1 cells and then imaged under the TIRF microscope. The degree of flashing was determined by Metamorph analysis. The domains of the proteins are as follows, K, kinase domain; N, N-terminal auxilin homology domain; P, PTEN-like domain; CB, clathrin-binding domain; J, J-domain. GAK and auxilin constructs are aligned so that their domain structures are homologous to one another. The number of GAK and auxilin flashes that occurred in a 300-mm^2 area of the cell over a 10-second time period was counted to obtain the values for the mean and s.d. from at least four cells.

uncoating, for clathrin exchange, for chaperoning dissociated clathrin and perhaps for facilitating the rebinding of clathrin and adaptor proteins to newly forming CCPs (Jiang et al., 2000; Yim et al., 2005; Lee et al., 2005). In addition, GAK and Hsc70 may be involved in constriction of the vesicle neck and scission of the CCVs from the membrane (Newmyer et al., 2003). Since GAK and auxilin are involved in many processes during clathrin-mediated endocytosis, they might be crucial for the cell to regulate the level of recruitment of these proteins.

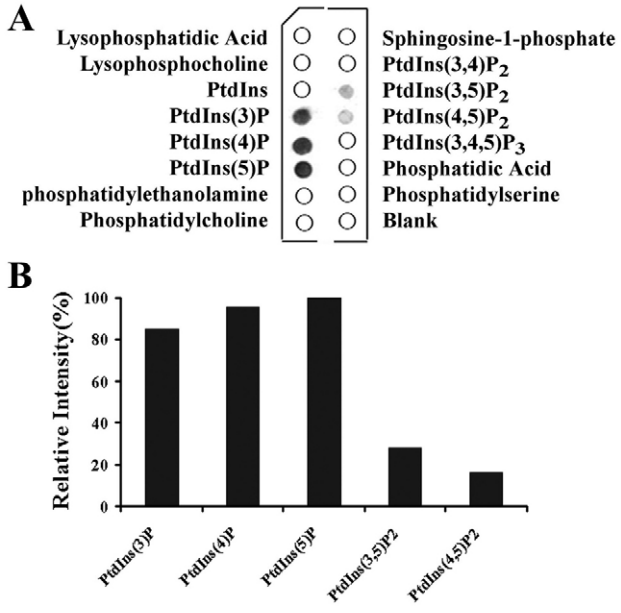

Fig. 8. Protein lipid overlay obtained using GST-PTEN-like domain of GAK. (A) Binding of GST-PTEN-like domain of GAK to phosolipids was measured using the protein lipid overlay strips. (B) Quantification of the phosolipid overlay. The binding to the phospholipids strip was performed as described in Materials and Methods. The circles along the periphery of the strip indicate the different phospholipids that were tested in the binding assay.

Our major finding in this study is that, following dynamin recruitment, there is a brief burst of GAK recruitment to the CCPs. Following this event, there is a loss of both clathrin and GAK from the evanescent field as the pit invaginates. Finally, both GAK and clathrin simultaneously disappear from the epifluorescent field, suggesting dissociation of the clathrin coat from the budded vesicle. The burst or rapid increase in GAK binding to the CCPs could recruit relatively high levels of Hsc70 resulting in irreversible uncoating of the CCVs. The burst of GAK binding also occurs at about the time of vesicle scission and, therefore, Hsc70 might also be involved in this process. It is less likely that Hsc70 is involved in constriction of the vesicle neck because the burst of GAK binding occurs after the level of dynamin starts to decline. However, dynamin might trigger the binding of GAK and this binding might then continue even after dynamin itself dissociates. In this regard, when we deleted the major dynamin-binding domain, there was a loss of GFP-GAK recruitment to the CCPs on the plasma membrane. However, this domain also has binding sites for clathrin and AP2 so it is not yet proven that it is the binding to dynamin that is crucial for GAK recruitment.

Interestingly, we found that recruitment of GAK to the CCPs was not sufficient by itself to cause budding and irreversible clathrin uncoating. GAK repeatedly flashed on clathrin puncta

Table 1. Effect of conditions on the flashing of GAK in HeLa and CV1 cells

Conditions	Flashes
Control	24±13
Dynamin 1	22±12
K44A dynamin 1	0
Cholesterol-depletion	0
K^+-depletion	2±3
Sucrose	1±1
AP2_ RNAi	0*
Clathrin_ RNAi	0*

Data were quantified as described in Fig. 7.
*This was measured in HeLa cells only.

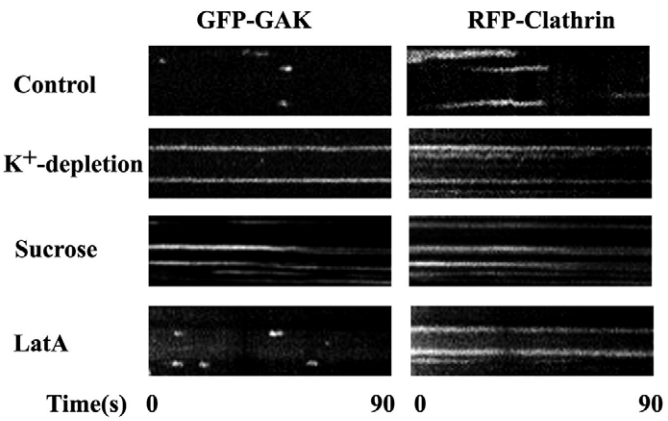

Fig. 9. Kymographs of GAK and mRFP-clathrin obtained under different experimental conditions. GFP-GAK and mRFP-clathrin were imaged simultaneously by TIRF microscopy. Kymographs were generated using Metamorph software by taking a rectangular region and assembling this region in a side-by-side chronological order to form a montage. TIRF images were acquired under following conditions: in medium (DMEM and FBS; Control) in K^+-depletion medium (K^+-depletion), in hypertonic sucrose solution (sucrose) and in medium containing 2.5 μM LatA.

in LatA-treated cells even though the fluorescence of the clathrin puncta did not decrease. Therefore, despite the repeated recruitment of high levels of GAK, neither scission of the CCVs or their irreversible uncoating occurred in the absence of actin activity.

The GAK flash requires the PTEN-like domain of GAK, which is the first time a role for this domain has been observed. It is likely that the function of the PTEN-like-domain is to bind to phosphate groups either on a lipid or a protein, enabling high local concentrations of GAK to accumulate on the CCPs. In this regard, we found that the PTEN-like domain preferentially binds to phosphoinositol monophosphates such as PtdIns(4)*P*. Therefore, one possibility is that large amounts of GAK are recruited to the CCPs when PtdIns(4,5)P_2 is hydrolyzed to PtdIns(4)*P* by synaptojanin. This proposal is consistent with the observation that synaptojanin knock-out mice show an accumulation of CCVs at synapses (Cremona et al., 1999). It is, therefore, possible that the binding of synaptojanin is required for recruitment of GAK, which in turn is required for irreversible clathrin uncoating. Alternatively, phosphorylation of one or more of the proteins on the clathrin-coated pits may be responsible for the wave of GAK recruitment. Most of the proteins comprising the CCPs are phosphorylated (Bar-Zvi et al., 1988) and the role of this phosphorylation is, in most cases, not yet understood.

Our in vitro experiments strongly suggest that Hsc70 and GAK are required for clathrin exchange as well as clathrin uncoating (Greener et al., 2000; Yim et al., 2005; Lee et al., 2005). Nevertheless, we were unable to detect GAK binding to CCPs in cells that expressed the K44A-dynamin mutant or were depleted of cholesterol even though clathrin exchange occurs in these cells. Apparently, the fluorescence intensity of the catalytic amounts of GAK required for exchange is too low to detect on CCPs above the background cytosolic GAK fluorescence. Interestingly, in hypertonic-sucrose-treated or K^+-depleted cells, in which clathrin is immobilized on CCPs, many cells showed GAK continuously bound to these CCPs. However, this continuous GAK binding is different from the transient binding that we observed when GAK flashes. In the former case, even GAK-truncation mutants that lack the PTEN-like domain continuously bound to the CCPs, whereas in the latter case the PTEN-like domain was required. It is possible that the low level of GAK binding that is required to catalyze clathrin exchange also occurs in the absence of the PTEN-like domain but further work will be required to determine whether this is the case.

Since we detected GAK on the CCPs, we also attempted to detect GFP-Hsp70 or the dominant-negative mutant of Hsp70, GFP-Hsp70(K71E) bound to CCPs (Zeng et al., 2004). We could not detect the binding of either Hsp70 or the Hsp70 mutant to CCPs under control conditions or in hypertonic-sucrose-treated or K^+-depleted cells, conditions in which GAK continuously binds to these pits. Perhaps, the background cytosolic Hsp70 fluorescence was too high to detect bound Hsp70 on the CCPs.

Summarizing the implications of our data for the mechanism of endocytosis, our results – in combination with the results of Merrifield and co-workers (Merrifield et al., 2005) – show that, large amounts of GAK are recruited to CCPs at about the same time as vesicle scission occurs and then, shortly after, clathrin-uncoating follows. Thus our results are consistent with the view that Hsc70 together with actin are involved in scission of the CCVs and also in irreversible clathrin uncoating. However, our results do not support the view that high levels of GAK and Hsc70 are involved in constriction of the vesicle neck because GAK and Hsc70 are recruited only after the level of dynamin is already decreasing. Of course, whereas recruitment of high levels of Hsc70 at the time of scission could mean it is involved in the scission event, it is also possible that this Hsc70 is only involved in the irreversible clathrin uncoating that occurs immediately after scission. As for the role of GAK in the clathrin exchange that occurs during invagination, it is still our view that GAK and Hsc70 are involved in this step, even though we were unable to detect on the pits the catalytic levels of GAK or Hsc70 that are required for reversible clathrin exchange. Therefore, more work will be required to confirm that low levels of GAK and Hsc70 are causing the clathrin exchange that occurs early in the endocytic cycle and, also, to determine how the high levels of GAK and Hsc70 recruited late in the endocytic cycle work with actin to cause vesicle scission and uncoating.

Materials and Methods

DNA constructs

Human GAK and bovine auxilin DNA were cloned into pEGFP-C1 vector (Clontech). Human clathrin light chain A (LCa) was subcloned into the *Xho*I and *Eco*RI sites of the monomeric red fluorescent protein mRFP-N1 vector from R. Tsien (UC San Diego, CA) (Campbell et al., 2002) or into DsRed fluorescent protein (Lee et al., 2005). GFP-dynamin1 (human isoform1 aa) obtained from P. De. Camilli (Yale University, CT) was subcloned into mRFP-C1. GFP-dynamin2 (rat isoform 2aa) was from Mark McNiven (Mayo Clinic, MN). HA-tagged dynamin1 wild-type and K44A vectors were obtained from Samuel Cushman (NIH, Bethesda, MD). Mutants of GAK and auxilin were made using the primers listed in Table S1 (supplementary material). The homology analysis for auxilin, GAK and PTEN was determined using the ClustalX 1.83 software program (Thompson et al., 1997).

Tissue culture

HeLa and CV1 cells were maintained in Dulbecco's modified Eagle's medium (DMEM; Biosource, MD, USA) supplemented with 10% fetal bovine serum (FBS;

Biosource, MD, USA), 2 mM glutamine, penicillin (100 units/ml) and streptomycin (100 units/ml) in a humidified incubator with 5% CO_2 at 37°C. Cells were transfected with the assorted plasmids using Fugene6 (Roche Diagnostics, IN). Confocal imaging of transfected cells with GFP-GAK, GFP-auxilin, and the mutants of GAK and auxilin showed that there was similar expression levels with the wild-type and mutant proteins. HeLa cells stably expressing wild-type and mutant (K44A) dynamin were grown under control of a tetracycline promoter in the presence of tetracycline (Sigma-Aldrich). These proteins were induced by removal of tetracycline (Damke et al., 1995). Hypertonic treatment, K^+-depletion, and cholesterol depletion was described previously (Wu et al., 2001). Cells were treated with 2.5 μM latrunculin A (LatA) (Sigma-Aldrich) for 30 minutes at 37°C (Wu et al., 2001).

HeLa cells were depleted of AP2 and clathrin by RNA interference (RNAi) using the identical small oligonucleotides and procedure of Robinson and co-workers (Motley et al., 2003). To insure that these proteins were depleted, we always checked there was a marked inhibition of transferring uptake of Alexa-Fluor-546-transferrin (Molecular Probes). Cells were fixed and stained for endogenous GAK using rabbit polyclonal GAK antibodies (Lee et al., 2005). Cells were fixed and stained the following antibodies were used: anti-AP1 (Sigma), anti-GGA3 (BD Biosciences), and anti-GM130 (BD Biosciences), anti-TGN46 (Serotec) and rabbit polyclonal GAK (Greener et al., 2000). Secondary antibodies used were Rhodamine-conjugated donkey anti-mouse IgG antibody and Cy5- conjugated goat anti-mouse IgM antibody (Jackson ImmunoResearch Laboratory Inc.).

Microscopy

The Olympus microscope was used with a 60 ×, 1.45 NA oil-immersion objective to obtain both evanescent and epifluorescent images (Lee et al., 2005). For evanescent images, GFP and mRFP were excited with the 488 nm line of an argon laser (Melles Griot, Carlsbad, CA) and the 567 nm line of a krypton laser (Melles Griot, Carlsbad, CA), respectively. Epifluorescence images were obtained using a mercury lamp. An image splitter (Optical Insights, Santa Fe, NM) was used to image both green and red fluorophores simultaneously. Green and red emissions were collected simultaneously using a Dual-View splitter (model 01-24-SEML1, Optical Insights, Santa Fe, NM, USA) equipped with a 565 dichroic filter to split the beam, a 525/50 band-pass filter to collect green emission, and a 605/55 filter to collect red emission. On the basis of single fluorophore control experiments, there was no detectable green to red bleed-through with GFP-GAK or GFP-auxilin into the mRFP-clathrin channel. Laser and mercury lights were applied through independent electronic shutters (Vincent Associates, Rochester, NY) to obtaining alternating epifluorescence and evanescent images. Cells incubated beforehand in Phenol-Red-free medium were imaged at 37°C, while controlling the temperature with a CTI Controller 3700 digital (Zeiss, Germany). Images were collected using a Photometrics Cool Snap HQ CCD camera (Photometrics, Tucson, AZ). Streams of 120 frames were exposed and acquired at 1 second per frame for 120 seconds. The Zeiss LSM510 live confocal microscope was used to obtain rapid imaging in 3D. The Zeiss LSM 510 was used for confocal microscopy.

Image analysis

Data sets were acquired and analyzed using Metamorph software (Universal Imaging, PA). When alternating epifluorescence and evanescent images were acquired, the images from each field were separated into stacks. Green and red images were aligned before separating them into individual stack files. A circle of 0.6 μm diameter (35 pixels) was drawn around a spot in the green channel (auxilin, GAK or dynamin) and then transferred to the corresponding region in the red channel (clathrin or dynamin) using Metamorph software function. The average fluorescence intensity was then calculated for the spot as a function of time. The data were exported to Microsoft Excel to generate graphs of time versus fluorescence intensity. The relative intensity was then normalized with the maximum and minimum intensity in the time series equated to 1.0 and 0, respectively. The time point at maximum intensity of the image obtained in the green channel (e.g. GFP-GAK or GFP-dynamin) was set to zero (t=0) in plotting the data. Data sets were averaged and the standard deviation (s.d.) was plotted for each data point. S.d. are used to show the spread of the distribution.

GST-protein preparation

E. coli BL21/DE3 (Invitrogen) cells were transformed with pGEX6P1 (Amersham Biosciences) encoding the GAK-PTEN-like domain construct. After induction of protein, the cells were lysed and purified using glutathione-agarose beads (Amersham Biosciences). GST-fusion proteins were eluted from the beads by incubation with 1 ml of glutathione elution buffer (10 mM reduced glutathione in 50 mM Tris-HCl, pH 8.0). The pooled eluate from three elutions of the column was dialyzed overnight against TBS buffer (10 mM Tris, 150 mM NaCl, pH 8.0).

Protein-lipid overlay

The PIP-strip membranes (Echelon) were blocked in TBS with 0.1% (v/v) Tween-20 (TBS-T) and 3% fatty-acid-free bovine serum albumin (BSA; (ICN Biochemicals) and gently agitated for 1 hour at room temperature. The membranes were incubated with 0.5 μg/ml protein of interest in TBS-T with 3% BSA for 1-4 hours at room temperature, and then washed with TBS-T with 3% BSA three times with gentle agitation for 10 minutes each. This wash step was repeated between all incubation steps and before detection. The GST detection module (Amersham Pharmacia) was used to detect GST-fusion proteins, followed by incubation with goat anti-IgG-HRP (KPL, Gaithersburg, MD) at 1:10,000 in TBS-T with 3% BSA. ECL detection (Amersham Biosciences) and Hyperfilm ECL (Amersham Biosciences) were used to detect the bound protein followed by imaging the film using the ChemiImager (Alpha Innotach, San Leandro, CA).

We thank Pietro DeCamilli (Yale University, New Haven, CT) for GFP-dynamin 1, Mark McNiven (Mayo Clinic, Rochester, MN) and Sandra Schmid (Sripps Institute, La Jolla, CA) for the HeLa cells stably expressing wild-type and K44A dynamin under the tetracycline promoter, Roger Tsien (UC San Diego, La Jolla, CA) for mRFP vector, Anthony Panzera for help in analyzing the data, and Xiaohong Zhao for invaluable technical assistance.

References

Bar-Zvi, D., Mosley, S. T. and Branton, D. (1988). In vivo phosphorylation of clathrin-coated vesicle proteins from rat reticulocytes. *J. Biol. Chem.* **263**, 4408-4415.

Campbell, R. E., Tour, O., Palmer, A. E., Steinbach, P. A., Baird, G. S., Zacharias, D. A. and Tsien, R. Y. (2002). A monomeric red fluorescent protein. *Proc. Natl. Acad. Sci. USA* **99**, 7877-7882.

Cremona, O., Di Paolo, G., Wenk, M. R., Luthi, A., Kim, W. T., Takei, K., Daniell, L., Nemoto, Y., Shears, S. B., Flavell, R. A. et al. (1999). Essential role of phosphoinositide metabolism in synaptic vesicle recycling. *Cell* **99**, 179-188.

Damke, H., Gossen, M., Freundlieb, S., Bujard, H. and Schmid, S. L. (1995). Tightly regulated and inducible expression of dominant interfering dynamin mutant in stably transformed HeLa cells. *Meth. Enzymol.* **257**, 209-220.

Ehrlich, M., Boll, W., Van Oijen, A., Hariharan, R., Chandran, K., Nibert, M. L. and Kirchhausen, T. (2004). Endocytosis by random initiation and stabilization of clathrin-coated pits. *Cell* **118**, 591-605.

Ford, M. G., Pearse, B. M., Higgins, M. K., Vallis, Y., Owen, D. J., Gibson, A., Hopkins, C. R., Evans, P. R. and McMahon, H. T. (2001). Simultaneous binding of PtdIns(4,5)P2 and clathrin by AP180 in the nucleation of clathrin lattices on membranes. *Science* **291**, 1051-1055.

Ford, M. G., Mills, I. G., Peter, B. J., Vallis, Y., Praefcke, G. J., Evans, P. R. and McMahon, H. T. (2002). Curvature of clathrin-coated pits driven by epsin. *Nature* **419**, 361-366.

Gaidarov, I., Santini, F., Warren, R. A. and Keen, J. H. (1999). Spatial control of coated-pit dynamics in living cells. *Nat. Cell Biol.* **1**, 1-7.

Greene, L. E. and Eisenberg, E. (1990). Dissociation of clathrin from coated vesicles by the uncoating ATPase. *J. Biol. Chem.* **265**, 6682-6687.

Greener, T., Zhao, X., Nojima, H., Eisenberg, E. and Greene, L. E. (2000). Role of cyclin G-associated kinase in uncoating clathrin-coated vesicles from non-neuronal cells. *J. Biol. Chem.* **275**, 1365-1370.

Haynie, D. T. and Ponting, C. P. (1996). The N-terminal domains of tensin and auxilin are phosphatase homologues. *Protein Sci.* **5**, 2643-2646.

Hinshaw, J. E. (2000). Dynamin and its role in membrane fission. *Annu. Rev. Cell Dev. Biol.* **16**, 483-519.

Jiang, R., Gao, B., Prasad, K., Greene, L. E. and Eisenberg, E. (2000). Hsc70 chaperones clathrin and primes it to interact with vesicle membranes. *J. Biol. Chem.* **275**, 8439-8447.

Keyel, P. A., Watkins, S. M. and Traub, L. (2004). Endocytic adaptor molecules reveal an endosomal population of clathrin by total internal reflection fluorescence microscopy. *J. Biol. Chem.* **279**, 13190-13204.

Lee, D. W., Zhao, X., Eisenberg, E. and Greene, L. E. (2005). Depletion of GAK/Auxilin 2 inhibits receptor-mediated endocytosis and recruitment of both clathrin and clathrin adaptors. *J. Cell Sci.* **118**, 4311-4321.

Merrifield, C. J., Feldman, M. E., Wan, L. and Almers, W. (2002). Imaging actin and dynamin recruitment during invagination of single clathrin-coated pits. *Nat. Cell Biol.* **4**, 691-698.

Merrifield, C. J., Qualmann, B., Kessels, M. M. and Almers, W. (2004). Neural Wiskott Aldrich Syndrome Protein (N-WASP) and the Arp2/3 complex are recruited to sites of clathrin-mediated endocytosis in cultured fibroblasts. *Eur. J. Cell Biol.* **83**, 13-18.

Merrifield, C. J., Perrais, D. and Zenisek, D. (2005). Coupling between clathrin-coated-pit invagination, cortactin recruitment, and membrane scission observed in live cells. *Cell* **121**, 593-606.

Moskowitz, H. S., Heuser, J., McGraw, T. E. and Ryan, T. A. (2003). Targeted chemical disruption of clathrin function in living cells. *Mol. Biol. Cell* **14**, 4437-4447.

Motley, A., Bright, N. A., Seaman, M. N. and Robinson, M. S. (2003). Clathrin-mediated endocytosis in AP-2-depleted cells. *J. Cell Biol.* **162**, 909-918.

Newmyer, S. L., Christensen, A. and Sever, S. (2003). Auxilin-dynamin interactions link the uncoating ATPase chaperone machinery with vesicle formation. *Dev. Cell* **4**, 929-940.

Rappoport, J. Z. and Simon, S. M. (2003). Real-time analysis of clathrin-mediated endocytosis during cell migration. *J. Cell Sci.* **116**, 847-855.

Rappoport, J. Z., Taha, B. W., Lemeer, S., Benmerah, A. and Simon, S. M. (2003). The AP-2 complex is excluded from the dynamic population of plasma membrane-associated clathrin. *J. Biol. Chem.* **278**, 47357-47360.

Rappoport, J. Z., Benmerah, A. and Simon, S. M. (2005). Analysis of the AP-2 adaptor complex and cargo during clathrin-mediated endocytosis. *Traffic* **6**, 539-547.

Roux, A., Uyhazi, K., Frost, A. and De Camilli, P. (2006). GTP-dependent twisting of dynamin implicates constriction and tension in membrane fission. *Nature* **441**, 528-531.

Scheele, U., Kalthoff, C. and Ungewickell, E. (2001). Multiple interactions of auxilin 1 with clathrin and the AP-2 adaptor complex. *J. Biol. Chem.* **276**, 36131-36138.

Schlossman, D. M., Schmid, S. L., Braell, W. A. and Rothman, J. E. (1984). An enzyme that removes clathrin coats: purification of an uncoating ATPase. *J. Cell Biol.* **99**, 723-733.

Thompson, J. D., Gibson, T. J., Plewniak, F., Jeanmougin, F. and Higgins, D. G. (1997). The CLUSTAL_X windows interface: flexible strategies for multiple sequence alignment aided by quality analysis tools. *Nucleic Acids Res.* **25**, 4876-4882.

Umeda, A., Meyerholz, A. and Ungewickell, E. (2000). Identification of the universal cofactor (auxilin 2) in clathrin coat dissociation. *Eur. J. Cell Biol.* **79**, 336-342.

Ungewickell, E., Ungewickell, H., Holstein, S. E., Lindner, R., Prasad, K., Barouch, W., Martin, B., Greene, L. E. and Eisenberg, E. (1995). Role of auxilin in uncoating clathrin-coated vesicles. *Nature* **378**, 632-635.

Wenk, M. R. and De Camilli, P. (2004). Protein-lipid interactions and phosphoinositide metabolism in membrane traffic: insights from vesicle recycling in nerve terminals. *Proc. Natl. Acad. Sci. USA* **101**, 8262-8269.

Wu, X., Zhao, X., Baylor, L., Kaushal, S., Eisenberg, E. and Greene, L. E. (2001). Clathrin exchange during clathrin-mediated endocytosis. *J. Cell Biol.* **155**, 291-300.

Wu, X., Zhao, X., Puertollano, R., Bonifacino, J. S., Eisenberg, E. and Greene, L. E. (2003). Adaptor and clathrin exchange at the plasma membrane and trans-Golgi network. *Mol. Biol. Cell* **14**, 516-528.

Yarar, D., Waterman-Storer, C. M. and Schmid, S. L. (2005). A dynamic actin cytoskeleton functions at multiple stages of clathrin-mediated endocytosis. *Mol. Biol. Cell* **16**, 964-975.

Yim, Y. I., Scarselletta, S., Zang, F., Wu, X., Lee, D. W., Kang, Y. S., Eisenberg, E. and Greene, L. E. (2005). Exchange of clathrin, AP2 and epsin on clathrin-coated pits in permeabilized tissue culture cells. *J. Cell Sci.* **118**, 2405-2413.

Zeng, X. C., Bhasin, S., Wu, X., Lee, J. G., Maffi, S., Nichols, C. J., Lee, K. J., Taylor, J. P., Greene, L. E. and Eisenberg, E. (2004). Hsp70 dynamics in vivo: effect of heat shock and protein aggregation. *J. Cell Sci.* **117**, 4991-5000.

Zhao, X., Greener, T., Al-Hasani, H., Cushman, S. W., Eisenberg, E. and Greene, L. E. (2001). Expression of auxilin or AP180 inhibits endocytosis by mislocalizing clathrin: evidence for formation of nascent pits containing AP1 or AP2 but not clathrin. *J. Cell Sci.* **114**, 353-363.